論文 / 著書情報
Article / Book Information

Title	Creep Deformation Measurement of Fiber-reinforced Plastic Materials for Industrial Robot Applications
Authors	Kenji Sekiguchi, Yuta Tsukamoto, Hiroyuki Nabae, Gen Endo
Citation	Proceedings of the 2025 IEEE/SICE International Symposium on System Integration, IEEE, , ,
Pub. date	2025, 1
Copyright	(c) 2025 IEEE. Personal use of this material is permitted. Permission from IEEE must be obtained for all other uses, in any current or future media, including reprinting/republishing this material for advertising or promotional purposes, creating new collective works, for resale or redistribution to servers or lists, or reuse of any copyrighted component of this work in other works.
DOI	http://dx.doi.org/10.1109/SII59315.2025.10871048
Note	This file is author (final) version.

Creep Deformation Measurement of Fiber-reinforced Plastic Materials for Industrial Robot Applications

Kenji Sekiguchi[1] , Yuta Tsukamoto[1], Hiroyuki Nabae[1], and Gen Endo[1]

***Abstract*— Replacing the metal structural parts with plastic structural parts will directly reduce energy consumption, thanks to their lightweight. However, plastic materials are prone to creep deformation at room temperature, potentially leading to decreased end-effector positioning accuracy during prolonged use. Previous measurements of creep deformation in lightweight plastics revealed significant deformation in 3D-printed parts, likely due to low infill rates and suboptimal reinforcement fiber placement. This paper presents the results of creep deformation measurements on test specimens with improved structural designs, including modified infill rates and fiber placements. The experimental results show that continuous carbon fiber placement along the outer wall direction yielded the least creep deformation. Additionally, variations in infill rates had minimal impact on creep deformation.**

I. INTRODUCTION

Industrial robots, known for their high precision, efficiency, and excellent reproducibility, are widely used to enhance productivity and quality in manufacturing. However, with the increasing focus on the Sustainable Development Goals and decarbonization efforts, there is a growing demand for energy conservation in the manufacturing sector. Industrial robots account for 8% of the total energy consumption in manufacturing [1] and approximately 60% of their overall operating costs [2]. Therefore, improving the energy efficiency of industrial robots is crucial not only for realizing a decarbonized society but also for reducing operational costs.

Various approaches have been proposed to reduce energy consumption in industrial robots. Hardware-based methods include lightweight design [3][4], while software-based approaches involve optimizing motion parameters [5] and developing energy-efficient motion planning [6][7]. However, software-based methods may have limited energy reduction effects for specific tasks and may not provide consistent results across different applications. Consequently, our research group has focused on a method of replacing metal components with plastic materials to achieve weight reduction in industrial robots. In previous studies, we developed a single-degree-of-freedom experimental apparatus using simplified robot link test specimens of different materials and an actuator with a harmonic drive. These experiments measured vibration damping characteristics [8] and compared stiffness properties when fastened [9], contributing to the study of suitable lightweight plastic materials for industrial robot structural components.

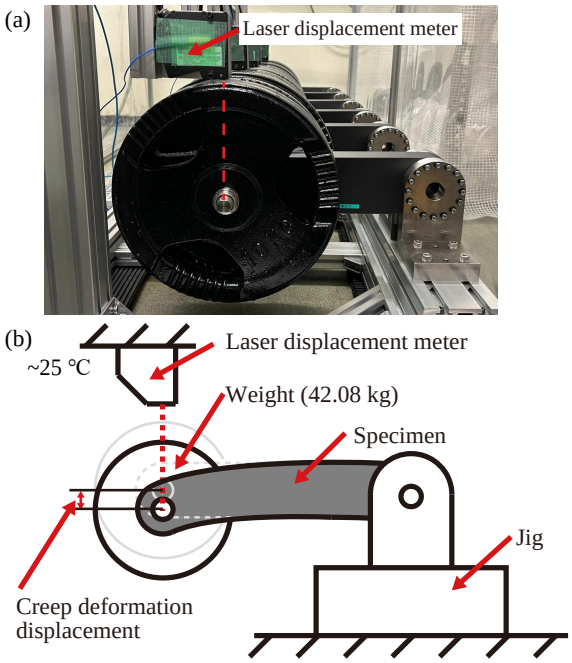

Fig. 1: (a) Experimental setup (b) Schematic diagram

This study focuses on creep deformation, a phenomenon where objects gradually deform under constant load. While metal materials generally do not exhibit creep deformation at room temperature, plastic materials do. This characteristic can lead to changes in the relative positions of manipulator joints during prolonged use, resulting in decreased end-effector positioning accuracy. However, if we can understand the trends and displacement magnitudes of creep deformation for specific plastic materials over time, we can implement periodic calibrations to mitigate accuracy degradation. Therefore, measuring creep deformation is crucial when considering suitable plastic materials for industrial robot structures. Previous studies have examined creep testing of common plastic materials such as polylactic acid (PLA) and acrylonitrile butadiene styrene (ABS) [10][11]. However, these studies used very small test specimens, making it uncertain whether their results can be applied to large-scale industrial robots. Consequently, there is a need to measure creep deformation under realistic link lengths and load conditions applicable to industrial robots. Our previous research on creep deformation measurement of plastic materials under cantilever beam end-point concentrated load conditions [12] revealed two issues.

*This research is subsidized by New Energy and Industrial Technology Development Organization (NEDO) under a project JPNP20016.

[1]All authors are with the Department of Mechanical Engineering, Institute of Science Tokyo. 2-12-1 Ookayama. Meguro-ku. Tokyo 152-8550. Japan. sekiguchi.k.ai. tsukamoto.y.ak. nabae.h.aa. endo.g.aa@m.titech.ac.jp

TABLE I: Propeties of 3D printed specimens

Material	Infill rate	CF arrangment	Molding time* (on Eiger)	Mass [g]	CF mount [cm^3] (on Eiger)	Cost [yen]
Onyx	37%	-	3d 8h	609.3	-	28,170
Onyx+CF	37%	4 layers each on front and back surfaces	2d 23h	646.0	24.69	34,600
Onyx+CF	37%	Outer wall 2 rings	3d 10h	682.8	81.27	47,400
Onyx+CF	55%	Outer wall 2 rings	4d 6h	878.8	81.27	56,230
Onyx+CF	55%	Outer wall 4 rings	4d 20h	943.9	155.5	72,160
Onyx+CF	55%	4 layers each on front and back surfaces	3d 18h	849.0	24.69	42,900
Onyx+CF	55%	8 layers each on front and back surfaces	3d 23h	870.5	49.40	46,900

(*Day is abbreviated as "d", and hour is abbreviated as "h")

Firstly, significant creep deformation was observed in 3D-printed test specimens. This was likely due to low infill rates and suboptimal placement of continuous carbon fiber (CF) reinforcement [12]. We hypothesize that structural improvements such as increasing infill rates or modifying CF placement could further suppress creep deformation. The advantages of 3D printing technology are ease of making free-form shapes and ease of weight reduction. If the above-mentioned structural improvements can achieve acceptable creep deformation, it is expected that 3D printed parts will be more applicable to industrial robot parts. Additionally, we will investigate discontinuous carbon fiber reinforced plastics, as there is a lack of research on creep deformation measurements under practical conditions with realistic link lengths and loads. These measurements are necessary to evaluate the applicability of these materials in industrial robot structures.

Secondly, drift calibration of the laser displacement meter for creep deformation measurements should be improved. Laser displacement meters are affected by measurement drift due to temperature changes. Although we applied drift calibration with the 100 hours preliminary experiment to the test results, ± 0.05 mm error persisted [12]. To obtain more accurate experimental data, we need to derive the drift rate per unit time from long-term preliminary experiments and apply it as a calibration value.

Therefore, this paper aims to achieve the following research objectives. Firstly, we will obtain more accurate measurement results by applying drift calibration derived from 200 hours preliminary experiments. Secondly, we will fabricate test specimens with varied infill rates and CF placements, as well as specimens made of discontinuous carbon fiber reinforced plastics. Using these specimens, we will quantitatively obtain the creep deformation in a cantilever beam configuration, as illustrated in Figure 1.

II. Specimen

Table I presents the material properties, infill rate, CF placement, fabrication time in Eiger, mass, CF quantity in Eiger, and cost for the test specimens. Eiger (Markforged Inc.) is the slicing software used in 3D printer. The first two rows of Table I show the characteristics of the specimens used in the previous creep test [12], included for comparison with the specimens used in the current experiment (rows 3-7). The 3D printing material Onyx+CF is a reinforced plastic consisting of Onyx (Markforged Inc.), a nylon plastic reinforced with short carbon fibers, further strengthened by the addition of continuous carbon fiber (CF) (F-FG-0005, Markforged Inc.). The specimens were fabricated using the X7 3D printer (Markforged Inc.). The fabrication parameters were set as follows: 0.125 mm layer pitch, triangular infill pattern, 8 solid layers, and 2 wall layers. These conditions are identical to those used in the previous creep test [12].

One of the factors contributing to the significant creep deformation observed in the previous creep test [12] was

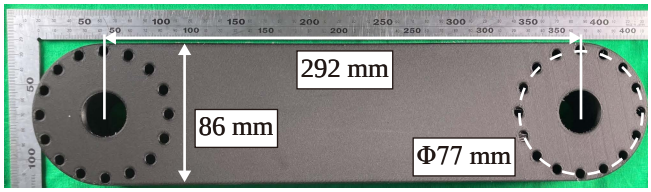

(a) Shape of the specimen

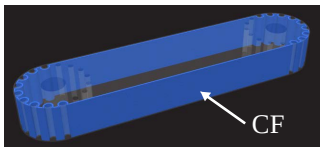

(b) Outer shell

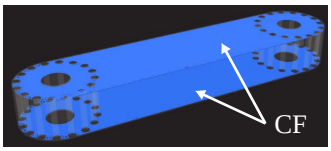

(c) Front and back surfaces

Fig. 2: Specimen

TABLE II: Mechanical propeties

Material	FELCARBO	Toughsite
Density [g/cm^3]	1.3	1.5
Tensile strength [MPa]	270	457
Tensile modulus [GPa]	22	33.2
Bending strength [MPa]	300	497
Bending modulus [GPa]	18	32.7
Fiber volume content [%]	approx. 30	50

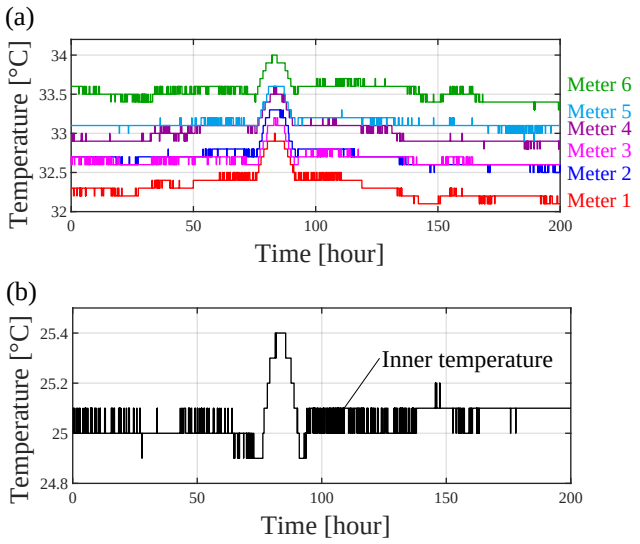

Fig. 3: The temperature measurement result of the drift calibration experiments (a) Head surface temperature of each laser displacement meter (b) Inner temperature

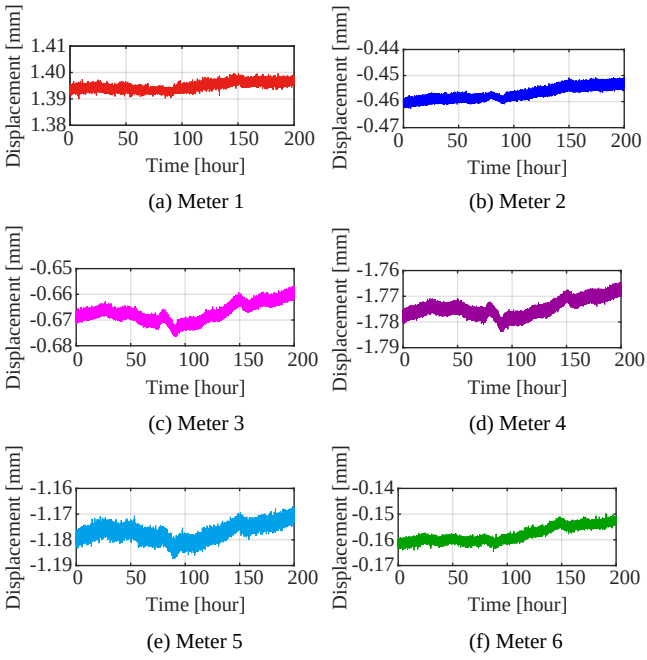

Fig. 4: The displacement result of the drift calibration experiments

the low infill rate of 37%. To investigate the impact of infill rate on creep deformation, we increased it to 55%, the maximum value configurable in Eiger. Figure 2 illustrates the specimen geometry and CF placement. All specimens were 45 mm thick, with CF placed in two configurations: along the outer wall direction as shown in Figure 2(b), and on the front and back surfaces as shown in Figure 2(c). As indicated in the second row of Table I, the previous creep test [12] only placed CF on the front and back surfaces of the specimen. This arrangement was parallel to the load direction and likely less contributed to suppress the creep deformation. Therefore, we placed CF perpendicular to the load direction along the outer walls and increased the number of CF layers in the surface direction to compare the effect of CF placement on creep deformation suppression.

The mechanical properties and fiber volume content of Toughsite and FELCARBO are shown in Table II. FELCARBO which showed minimal creep deformation in our previous creep test [12], is included for comparison with Toughsite. FELCARBO is a thermosetting plastic material manufactured by layering non-woven carbon fiber sheets, high-pressure molding, and machining. The volume content of carbon fibers in this material is approximately 30%. Unlike conventional carbon fiber reinforced plastics (CFRP), it exhibits high machinability and mechanical properties close to those of isotropic materials [13]. Toughsite, the subject of this study, is a random carbon fiber reinforced thermoplastic (CFRTP) composite. It is manufactured by layering sheets composed of chopped carbon fibers (approximately 5 mm in width and 20 mm in length) and nylon plastic, followed by thermal press molding. The volume content of carbon fibers is 50%. This manufacturing process results in excellent formability of the material [14].

TABLE III: Measured displacement drift calibration

Meter No.	Drift [μm/100 hour]
1	1.8
2	4.0
3	3.8
4	3.6
5	2.5
6	4.6

III. Creep Deformation Measurement

A. Experimental Apparatus

We used an experimental apparatus with a cantilever beam end point concentrated load structure, as shown in Figure 1. A weight of 42.08 kg was applied at a distance of 292 mm from the fixed end, and the creep deformation of the specimen was measured using a laser displacement meter (Keyence Co., Ltd., LK-H150, LK-G5000). In the case of industrial robot operation, the applied force vector at the end point of the arm is not constant. However, this experimental setup assumes a severe case where the robot maintains a posture with the highest joint torque. In addition, this setup simulates an industrial robot with a maximum reach of 1000 mm lifting a 12.3 kg weight in a horizontally extended posture. The load was applied using four weights of 10.52 kg each (total 42.08 kg), adjusted with additional weights for attachment. A collar was inserted between the weight and the center of the specimen, fixed with a shaft. Fine U-NUT (Fuji Seimitsu) were attached to both ends of the shaft to constrain the axial movement.

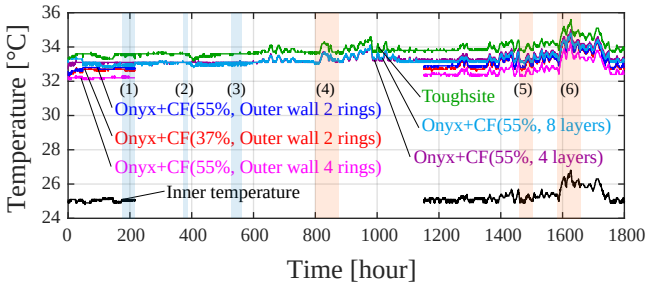

Fig. 5: The temperature measurement result of the experiment

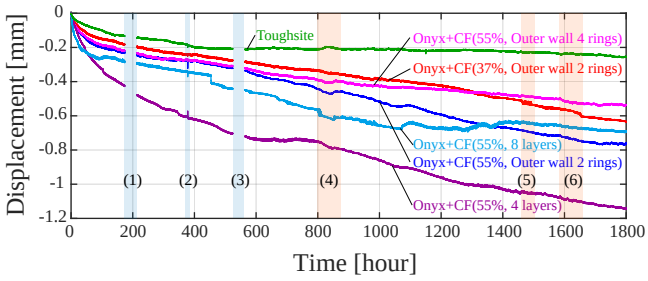

Fig. 6: Creep deformation measurement result with drift calibration

The fixed end of the specimen was secured to a stainless steel jig using M4 screws through 16 equally spaced through-holes, with a tightening torque of 3.6 Nm. For Onyx+CF specimens, we applied the bearing joint method proposed by our research group [15]. This method involves inserting a thin-walled metal cylindrical pipe into the plastic component when fastening soft plastic parts to metal parts, with the screw passing through the pipe coaxially. This approach prevents a decrease in fastening force and denting of the plastic part by having the thin-walled pipe bear the axial force of the screw. The through-holes in the Onyx+CF specimens were 6.2 mm in diameter, with SUS304 thin-walled cylinders (4.0 mm inner diameter, 1.0 mm wall thickness) inserted. Screws were then passed through the cylinders for fastening. For Toughsite specimens, 4.2 mm diameter through-holes were used, with screws inserted directly for fixing. This direct fastening method was chosen for Toughsite based on preliminary experiments that showed negligible small deformation around the through-holes when directly fixed with screws.

B. Temperature Management

Temperature changes affect not only creep deformation but also laser displacement meter measurements. Therefore, we installed a thermal insulation chamber around the test apparatus and maintained the internal temperature at 25°C. This temperature was chosen as it represents a typical room temperature for industrial robot operation. To manage the temperature, we first used the air conditioning system to lower the temperature in our experiment room to 22°C. Then, we installed a heater, fan, and thermocouple inside the insulation chamber. By circulating warm air with the fan and using feedback from the thermocouple, we maintained the internal temperature at 25°C. We measured the laser displacement meter head surface temperature using a thermocouple attached to the head surface. Similarly, we measured the chamber's internal temperature using a thermocouple.

C. Measurement Procedure

The measurement procedure was as follows.

1) Attach the specimen to the fixing jig using M4 screws with a tightening torque of 3.6 Nm, then mount it on the test apparatus.
2) Attach the weight to the specimen's tip while supporting it with a jack.
3) Turn on the temperature control equipment and wait for the internal temperature to stabilize at 25°C.
4) Turn on the laser displacement meter and wait for at least 4 hours.
5) Start the temperature and laser displacement measurements simultaneously, then remove the supporting jack to begin the test.

IV. Drift Calibration

Laser displacement meters are prone to measurement drift due to temperature changes, with drift amounts varying between individual meters. Therefore, it was necessary to measure the drift amount under temperature-controlled conditions. As a preliminary experiment, we measured the upper surface of a fixed aluminum frame. We collected time-series data of the fixed aluminum frame's surface displacement, the chamber's internal temperature, and the laser displacement meter head surface temperature over 200 hours (about 8 days). This duration is approximately twice that of the preliminary experiment conducted in our previous creep test [12]. Figure 3 shows the time-series changes in each laser displacement meter's head surface temperature and the chamber's internal temperature. We confirmed that the surface temperature changes of each laser displacement meter were within 0.6°C, and the internal temperature changes were within 0.4°C, which are negligible deviations. Figure 4 shows the time-series changes in displacement obtained by each laser displacement meter. The results confirmed drift over time. We performed least-squares approximation to determine the drift amount per unit time, as shown in Table III, and applied these values as calibration factors to our main test results.

V. Experiment Results

Figure 5 shows the measurement results of the internal chamber temperature and the laser displacement meter head surface temperature. Due to a malfunction in the temperature control equipment, time-series data for the chamber temperature and the three laser displacement meter head surface temperatures were lost from approximately 200 to 1100 hours. A strong correlation between the chamber temperature and head surface temperature was confirmed, suggesting that the temperature deviation remained below about 1.7°C throughout the 1800-hour measurement. This variation was

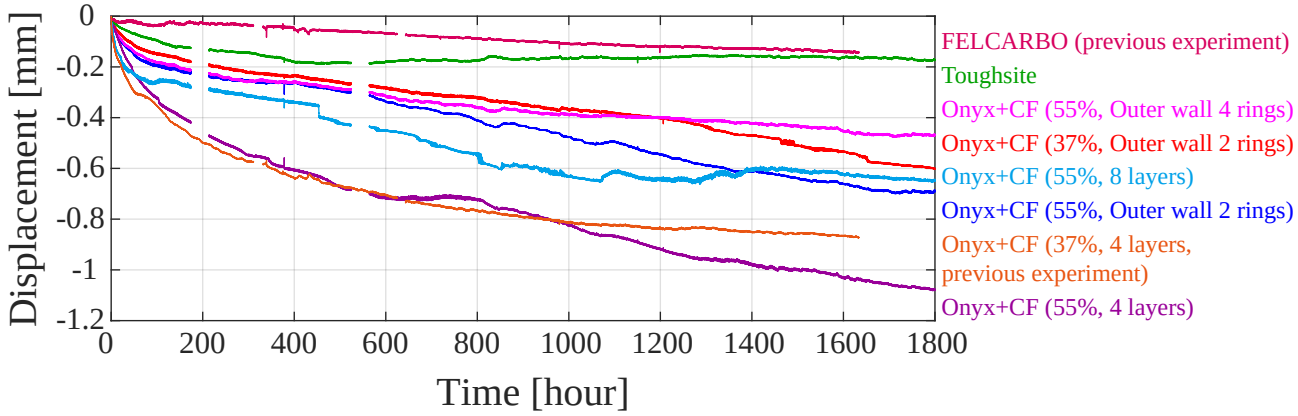

Fig. 7: Creep deformation measurement result without drift calibration

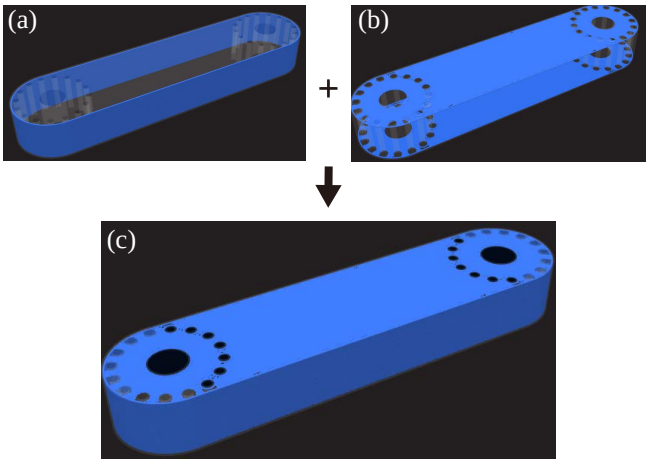

Fig. 8: Proposal for optimal placement of CF

larger compared to the preliminary experiment, which had temperature fluctuations below 0.4°C. In particular, rapid temperature changes occurred in the orange regions (4)(5)(6) of Figure 5, necessitating consideration of temperature-induced displacement measurement errors. These variations were primarily due to differences in ambient temperature. The drift calibration experiment was conducted in February when the ambient temperature was lower than the target. In contrast, the main experiment was carried out from March to May, when the ambient temperature was often close to the target. While the laboratory temperature was maintained at about 22°C by the building's air conditioning, the experimental temperature control equipment lacked cooling capabilities, making it susceptible to external air conditioning influences.

Figure 6 presents the 1800-hour displacement measurement results with laser displacement meter drift calibration applied. The baseline was set 15 minutes after removing the jack supporting the weights, as this process took several minutes. Data loss occurred in the light blue regions (1)(3) of Figure 6 due to unexpected updates on the data storage PC. The light blue region (2) shows minor vibrations caused by an earthquake. Figure 7 displays the 1800-hour displacement measurement results without laser displacement meter drift calibration. For comparison, we included uncorrected time-series data for FELCARBO and Onyx+CF (37% infill rate, CF placed in 4 layers on both surfaces) from our previous creep deformation measurement of plastic materials [12].

Comparing CF placement in the outer wall direction versus front and back surfaces, Figures 6 and 7 indicate that outer wall placement resulted in smaller deformation. The specimen with four CF rings in the outer wall direction showed the least creep deformation, measuring 0.53 mm after 1800 hours. This is likely due to the CF being perpendicular to the load direction, contributing to suppress the creep deformation.

No clear difference in creep deformation was observed due to varying infill rates. This suggests that CF placement was more dominant in suppressing creep deformation under 40 kgf load than increasing infill rate. While the maximum infill rate for our specimens was 55%, higher rates could be achieved by altering the infill pattern. However, increasing infill rate may not be practical for industrial robot applications as it would increase structural component weight, contradicting the goal of lightweight design. Table I also highlights issues such as increased manufacturing costs due to higher material usage and reduced productivity from longer fabrication times. Therefore, optimizing CF placement appears more effective in suppressing creep deformation than increasing infill rate.

One approach could be placing CF in both the outer wall direction and on front and back surfaces, as shown in Figure 8(c). The specimens used in this test had CF placed around the through-holes, as illustrated in Figure 2(b), due to the narrow space between the through-holes and side surfaces. Ideally, CF placement as shown in Figure 8(a) would be preferable. Adding CF to the front and back surfaces, as in Figure 8(b), could create a synergistic effect, further suppressing creep deformation.

Figure 6 shows that Toughsite's creep deformation after 1800 hours was 0.26 mm. Figure 7 indicates that its creep deformation was almost identical to FELCARBO. The accuracy of the laser displacement meter used in this experimental setup is expected to include an error of about 0.2 mm. Therefore, it is impossible to argue whether FELCARBO or Toughsite has less creep deformation.

VI. CONCLUSION

This study used an experimental apparatus to measure creep deformation under cantilever beam concentrated load conditions. We used Onyx+CF specimens with varied CF placement and Toughsite as test specimens. We quantitatively obtained the amount of creep deformations by experiments. The results showed that Toughsite exhibited less creep deformation compared to Onyx+CF. Among Onyx+CF specimens, those with CF placed in the outer wall direction showed less creep deformation, likely due to the CF being perpendicular to the load direction. No clear difference in creep deformation was observed due to varying infill rates. Despite occasional displacement measurement errors caused by rapid temperature changes, we successfully quantified the main long-term creep deformation trends.

As future work, it is necessary to conduct measurements using more accurate measuring apparatus and to evaluate the performance of the entire robot using plastic materials.

ACKNOWLEDGMENT

This research is subsidized by New Energy and Industrial Technology Development Organization (NEDO) under a project JPNP20016. This paper is one of the achievements of joint research with ROBOT Industrial Basic Technology Collaborative Innovation Partnership (ROBOCIP). Toughsite test specimens were provided by Professor Masahiro Arai (Nagoya University). We also thank Prof. Naoyuki Takesue (Tokyo Metropolitan University), Prof. Yusuke Ohta (Chiba Institute of Technology), and Prof. Takeshi Takaki (Hiroshima University) for their valuable comments.

REFERENCES

[1] M. Brossog, M. Bornschlegl, J. Franke, "Reducing the energy consumption of industrial robots in manufacturing systems. " Int. J. Adv. Manuf. Technol., 78 (2015), pp. 1315-1328

[2] F. Stuhlenmiller, J. Jungblut, D. Clever and S. Rinderknecht, "Combined Analysis of Energy Consumption and Expected Service Life of a Robotic System," 2020 6th International Conference on Mechatronics and Robotics Engineering (ICMRE), Barcelona, Spain, 2020, pp. 53-57, doi: 10.1109/ICMRE49073.2020.9065180.

[3] H. Yin, J. Liu and F. Yang, "Hybrid Structure Design of Lightweight Robotic Arms Based on Carbon Fiber Reinforced Plastic and Aluminum Alloy," in IEEE Access, vol. 7, pp. 64932-64945, 2019, doi: 10.1109/ACCESS.2019.2915363.

[4] X. Wang, D. Zhang, C. Zhao, P. Zhang, Y. Zhang and Y. Cai, "Optimal design of lightweight serial robots by integrating topology optimization and parametric system optimization", Mech. Mach. Theory, vol. 132, pp. 48-65, Oct. 2018.

[5] A. Rassõlkin, H. Hõimoja and R. Teemets, "Energy saving possibilities in the industrial robot IRB 1600 control", Proc. 7th Int. Conf.-Workshop Compat. Power Electron., pp. 226-229, 2011.

[6] O. Wigstrom, B. Lennartson, A. Vergnano and C. Breitholtz, "High-Level Scheduling of Energy Optimal Trajectories," in IEEE Transactions on Automation Science and Engineering, vol. 10, no. 1, pp. 57-64, Jan. 2013, doi: 10.1109/TASE.2012.2198816.

[7] X. Li, Y. Lan, P. Jiang, H. Cao and J. Zhou, "An Efficient Computation for Energy Optimization of Robot Trajectory," in IEEE Transactions on Industrial Electronics, vol. 69, no. 11, pp. 11436-11446, Nov. 2022, doi: 10.1109/TIE.2021.3118367.

[8] T. Takaki, M. Kanekiyo and G. Endo, "Damping Characteristics in Adaptation of Plastics for Robot Structures," 2023 IEEE/SICE International Symposium on System Integration (SII), Atlanta, GA, USA, 2023, pp. 1-4, doi: 10.1109/SII55687.2023.10039233.

[9] N. Takesue and Y. Ode, "Stiffness Model of Single-Geared Joint with 3D-Printed Link in Robot Arm," 2023 IEEE/SICE International Symposium on System Integration (SII), Atlanta, GA, USA, 2023, pp. 1-6, doi: 10.1109/SII55687.2023.10039160.

[10] T. Tezel, V. Kovan, E.S. Topal, "Effects of the printing parameters on short-term creep behaviors of three-dimensional printed polymers," J. Appl. Polym. Sci., 136 (21) (2019), Article 47564

[11] H. Zhang, L. Cai, M. Golub, Y. Zhang, X. Yang, K. Schlarman, et al. "Tensile, creep, and fatigue behaviors of 3D-printed acrylonitrile butadiene styrene, " J Mater Eng Perform, 27 (2018), pp. 57-62, 10.1007/s11665-017-2961-7

[12] Y. Tsukamoto, K. Sekiguchi, H. Nabae and G. Endo, "Measurement of Creep Deformation of Resin Structural Parts for a Lightweight Industrial Robot," 2024 IEEE/SICE International Symposium on System Integration (SII), Ha Long, Vietnam, 2024, pp. 592-597, doi: 10.1109/SII58957.2024.10417463.

[13] (Accessed: Aug 13. 2024) Futaba Corporation. " FELCARBO " . https://www.cfrp.mtb.futaba.co.jp/en/felcarbo

[14] (Accessed: Aug 6. 2024)FUKUVI CHEMICAL INDUSTRY CO.,LTD. " Toughsite " . hhttps://cfrp-toughsite.com/cfrtp/

[15] G. Endo, Y. Tsukamoto, H. Nabae and T. Takaki, "Proposal of a Fastening Method for Deformable Plastic Parts and Rigid Metal Parts," 2023 IEEE/SICE International Symposium on System Integration (SII), Atlanta, GA, USA, 2023, pp. 1-6, doi: 10.1109/SII55687.2023.10039451.